# Simulation of Boundary Layer Effects in the Pulse Tube of a Miniature Cryocooler

**T.J. Conrad[1], S.M. Ghiaasiaan[1], C.S. Kirkconnell[2]**

[1]Georgia Institute of Technology, Atlanta, GA USA
[2]Iris Technology Corporation, Irvine, CA USA

## ABSTRACT

As pulse tube cryocoolers are miniaturized, boundary layer effects in the pulse tube may become more important than they are for larger refrigerators. Nearly uniform flow in the pulse tube is necessary for efficient cooling, and this condition is compromised as the pulse tube diameter becomes smaller relative to the thermal and viscous boundary layer thicknesses. As a result, miniature pulse tube cryocoolers are likely to experience enhanced acoustic streaming losses compared to larger PTC's. This acoustic streaming results from thermal and viscous interactions between the working fluid and the pulse tube walls. The thermal and viscous penetration depths and their magnitudes relative to the pulse tube diameter and wall thickness are therefore important parameters for this phenomenon.

A parametric study of the effects of the pulse tube diameter, scaled to a non-dimensional value by the relevant boundary layer thicknesses, on acoustic streaming in the pulse tube was performed using CFD modeling. The effect of the operating frequency was also considered through the frequency dependence of the viscous and thermal penetration depths. Temperature dependant material properties were included in the CFD models because they play an important role in acoustic streaming. Results indicated that close attention must be paid to the sizes of the boundary layers relative to the pulse tube physical dimensions when designing miniature pulse tube cryocoolers.

## INTRODUCTION

The seminal pulse tube research done by Gifford and Longsworth in the 1960s concerned the use of low frequency (~1 Hz) pulse tubes which generated refrigeration through a surface heat pumping effect involving thermal interaction between the pulse tube working gas and the walls of the pulse tube.[1] This concept, which came to be called the Basic Pulse Tube Refrigerator (BPTR), was superseded in 1983 by Mikulin, *et al.*[2] through the invention of the much more efficient Orifice Pulse Tube Refrigerator (OPTR). The OPTR operates on a fundamentally different refrigeration process in which net enthalpy flow from the cold to the hot end is achieved by creating the proper phase shift between mass flow and pressure at the hot end of the pulse tube. The BPTR surface heat pumping refrigeration mechanism was recognized long ago as a *loss* mechanism in the OPTR.[3] Operation at higher frequency mitigates this loss as the period of oscillation becomes an increasingly small fraction of the pulse tube wall thermal time constant. In order to achieve the required

phase shift, the Mikulin OPTR was operated in the 5 to 10 Hz range. Subsequent maturation of the OPTR and the related inertance pulse tube refrigerator (IPTR) into full production of pulse tube cryocoolers has proceeded along with an increase in operating frequency. Typical operating frequencies for pulse tube cryocoolers today are in the range of 50 Hz and higher.

With surface heat transfer interactions along the walls of the pulse tube recognized as a loss mechanism, the ideal OPTR/IPTR performance is described by a simple 1-D enthalpy flow model in which boundary layer effects are neglected.[3] Momentum and enthalpy streaming losses along the pulse tube wall are known to occur due to boundary layer effects,[4] but these are typically small losses (<10% gross refrigeration capacity) in well designed "macro" pulse tube cryocoolers. That is because the 1-D approximation is reasonable for typical macro pulse tubes because the high operating frequency yields a boundary layer thickness that is negligible compared to the pulse tube diameter.

The drive towards miniaturization of pulse tube cryocoolers is leading to very small pulse tube diameters on the order of 2 mm, or less. As the pulse tube diameter gets smaller, at some point the assumption of negligible boundary thickness completely breaks down. Thus this drive to miniaturization is now challenging the 25 year old assumption that pulse tube boundary layer-to-wall interactions can be neglected, or at least treated as only a secondary loss mechanism.

Numerical experiments have been performed to investigate the characteristics and influence of the boundary layer in miniature pulse tubes. The drive down in size obviously exacerbates any concerns relating to a non-negligible boundary thickness. However, the characteristically higher frequencies (>150 Hz) of these cryocoolers is believed to be an ameliorating factor. In the sections to follow, computational fluid dynamics results are presented that provide some insight into how these competing factors balance in a prototypical miniature pulse tube cryocooler.

## MODEL METHODOLOGY

### Geometry and Boundary Layer Scaling

Geometry for the miniature pulse tube models was determined from typical dimensions of miniature PTC's[5-7] and scaling with regard to the boundary layer thicknesses. For the oscillatory flow occurring in the pulse tube, the relevant boundary layer thicknesses are the thermal and viscous penetration depths $\delta_T$ and $\delta_V$. The orders of magnitude of these are defined in Eq. 1 and 2, respectively, where k is the thermal conductivity, $\mu$ the dynamic viscosity, $\rho$ the density and $C_p$ the specific heat of the working fluid. Frequency dependence of the boundary layer thicknesses enters the equations through $\omega$, the angular frequency.

$$\delta_T = \sqrt{\frac{2k}{\omega \rho C_p}} \tag{1}$$

$$\delta_V = \sqrt{\frac{2\mu}{\omega \rho}} \tag{2}$$

The models incorporated helium as their working fluid. Temperature dependent properties, expected to enhance streaming phenomena in the pulse tube, were specified for the thermal conductivity, viscosity, and specific heat using tabular values at the operating pressure of 4 MPa.[8] The density was calculated using the ideal gas equation of state. Mean values of the thermal and viscous penetration depths, evaluated for helium at the mean temperature of 240 K, are shown in Table 1 for frequencies of 100, 200, 300 and 400 Hz. Pulse tube diameters of 1, 2, and 4 mm were chosen and modeled at each frequency, resulting in a wide range of the parameters $\delta_T/D$ and $\delta_V/D$ for the set of models. Values of $\delta_T/D$ and $\delta_V/D$ are presented for 240 K in Table 2.

Once the pulse tube inner diameters were determined by scaling with the boundary layer thicknesses, the remaining model geometry was chosen to be representative of typical miniature PTRs. Pulse tube lengths of 20 mm and warm and cold heat exchanger lengths of 5 mm were used for all of the models, regardless of diameter. Similarly, thicknesses of 0.25 mm were used for the pulse tube and heat exchanger walls.

**Table 1.** Thermal and viscous penetration depths for helium at 4 MPa and 240K.

| | Penetration Depths (mm) | |
|---|---|---|
| f (Hz) | Thermal | Viscous |
| 100 | 0.103 | 0.084 |
| 200 | 0.073 | 0.059 |
| 300 | 0.060 | 0.048 |
| 400 | 0.052 | 0.042 |

**Table 2.** Values of $\delta_T/D$ and $\delta_V/D$ for the investigated frequencies and pulse tube diameters at 240 K.

| | Pulse Tube Diameter (mm) | | | | | |
|---|---|---|---|---|---|---|
| | 1 | | 2 | | 4 | |
| f | $\delta_T/D$ | $\delta_V/D$ | $\delta_T/D$ | $\delta_V/D$ | $\delta_T/D$ | $\delta_V/D$ |
| 100 | 0.103 | 0.084 | 0.052 | 0.042 | 0.026 | 0.021 |
| 200 | 0.073 | 0.059 | 0.037 | 0.030 | 0.018 | 0.015 |
| 300 | 0.060 | 0.048 | 0.030 | 0.024 | 0.015 | 0.012 |
| 400 | 0.052 | 0.042 | 0.026 | 0.021 | 0.013 | 0.010 |

**Fluent Modeling**

Detailed representation of the characteristics of the boundary layer in a miniature pulse tube requires a multi-dimensional model with very fine grid spacing. In this investigation the Fluent CFD package[9] was used for all of the miniature pulse tube models. Commercial CFD packages such as Fluent have been shown to be capable of detailed solutions of models encompassing very complex geometries in two or three dimensions. Furthermore, recent successful simulations of cryocooler systems using CFD tools[5] have shown that such models can provide useful performance predictions for pulse tube refrigerators.

A schematic of the miniature pulse tube CFD models is shown in Figure 1. For computational efficiency, only the cold heat exchanger, pulse tube, and warm heat exchanger were included in the models. The symmetry of the problem was also taken advantage of with the use of 2-D axisymmetric models. Additional open fluid domains with initial lengths of 2 mm were added outside the two heat exchangers for the implementation of flow boundary conditions. The side walls of these domains were prescribed sinusoidal motions, shown in Figure 1, whose amplitudes A and B and phase angle f were adjusted to produce the desired oscillatory flow conditions in the pulse tube. These parameters were selected to provide a pressure ratio of 1.10, pulse tube gas column of 92%, and phase angles of 8° and 46° at the cold end and warm end of the pulse tube, respectively. The pulse tube gas column is the percentage of the gas contained in the pulse tube which does not leave it over the
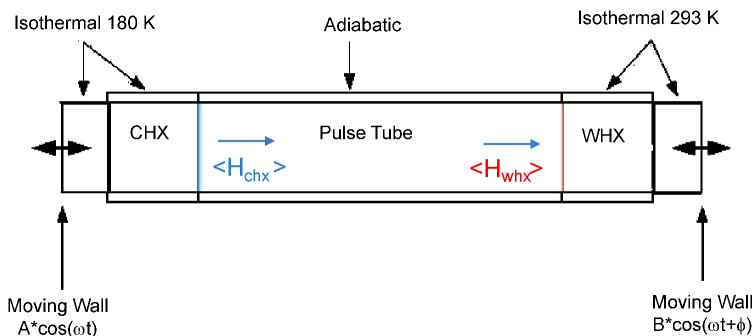


**Figure 1.** Schematic of miniature pulse tube models.

course of the oscillatory flow cycle. It is indicative of the combined oscillatory mass flow rates at both ends of the pulse tube, but unlike the mass flow rates may be held constant as the model scale changes. The phase angles are defined such that a positive phase angle indicates the pressure wave-form leading the velocity waveform. These operating conditions were similar to those predicted by full system CFD models of miniature PTCs.[10]

The moving walls and adjacent open zones used a dynamic meshing scheme which added and subtracted mesh layers as the wall moved. As shown in Figure 1, the outside walls of these open zones and the outer surfaces of the solid heat exchanger walls were isothermal. Temperatures of 293 K and 180 K were used at the warm and cold ends of the pulse tube, respectively. The moving walls were modeled as adiabatic because this improved the model convergence and simplified post pro-cessing. The outer surface of the pulse tube wall was also adiabatic. The pulse tube walls were modeled as steel and the heat exchanger walls were modeled as copper using constant material properties. These solid regions were discretized and included in order to incorporate wall conduc-tion into the models. Fluent's porous media model was used for the warm and cold heat exchangers, with viscous and inertial resistance coefficients related to the Darcy permeability and Forchheimer's inertial coefficient specified for #325 phosphor-bronze mesh at 67% porosity.[11]

The Fluent simulations used PRESTO! pressure discretization, PISO pressure-velocity cou-pling, and second order upwind discretization of all other quantities; these settings were chosen to provide the best and fastest convergence of the models. Double precision, pressure-based steady and unsteady solvers were used. Residual convergence criteria were set at $10^{-8}$ for the energy equa-tion, continuity, and axial and radial velocities. The models were initialized with a linear tempera-ture gradient using the steady-state solver, then iterated with the transient solver until they ap-proached periodic steady state. The time step size was selected to provide 250 time steps per period of oscillations for all four frequencies and the models were iterated for 2500 time steps (10 periods) before results were evaluated.

## RESULTS

The performance of the miniature pulse tube models was evaluated by comparing their net and gross cooling rates to those of corresponding 'ideal' models. The ideal models had adiabatic inter-nal pulse tube walls and viscosities which were artificially reduced by a factor of 1000. All other boundary conditions and model parameters were unchanged. This resulted in models which were essentially one-dimensional with negligible boundary layer effects. This is demonstrated in the velocity profiles shown in Figure 2 and the temperature profiles shown in Figure 3.

Figure 2 shows simulated instantaneous profiles of axial velocity for a cross section located at the midpoint of the pulse tube. Profiles are shown for the 200 Hz, 2 mm diameter ideal case and three $\delta_V/D$ values corresponding to the 200 Hz cases for each of the three pulse tube diameters. The radial position was scaled to a non-dimensional number using the pulse tube inner radius to com-pare results from the different diameter models on the same plot. The profiles displayed correspond to a time step at which the mass flow rate at the warm end of the pulse tube is at its cyclical maximum. Due to the phase shift occurring across the pulse tube, however, this is not exactly the time step corresponding to maximum velocity at the midpoint of the pulse tube and so the begin-ning of the flow reversal can be seen in the profile. The simulated results show nearly uniform flow for the ideal case and increasing viscous boundary layer thickness relative to the diameter as $\delta_V/D$ increases, indicating qualitative agreement of the model predictions with theory.

Similarly, Figure 3 shows simulated instantaneous profiles of temperature for the same cross section and time step. The ideal case is presented along with the same 200 Hz cases presented in the velocity profiles, although in this figure the models are identified by their $\delta_T/D$ values. Figure 4 shows contours of simulated temperature for the 2 mm diameter, 200 Hz ideal and standard models. From these two figures it can be seen that the ideal case has a nearly uniform predicted radial temperature distribution while thermal boundary layers are apparent for the non-ideal models. As was the case with the velocity profiles, the relative thickness of the simulated thermal boundary layer with respect to the diameter increased along with the $\delta_T/D$ parameter, again indicating model results in qualitative agreement with theoretical predictions.
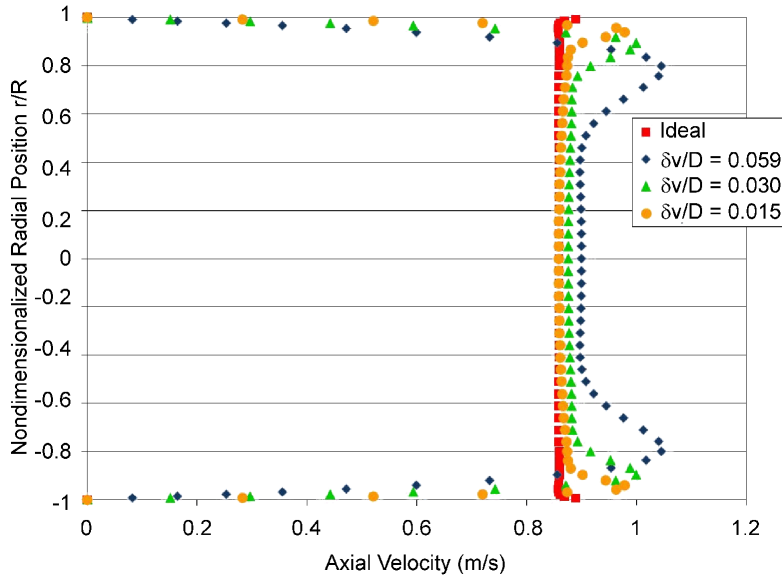
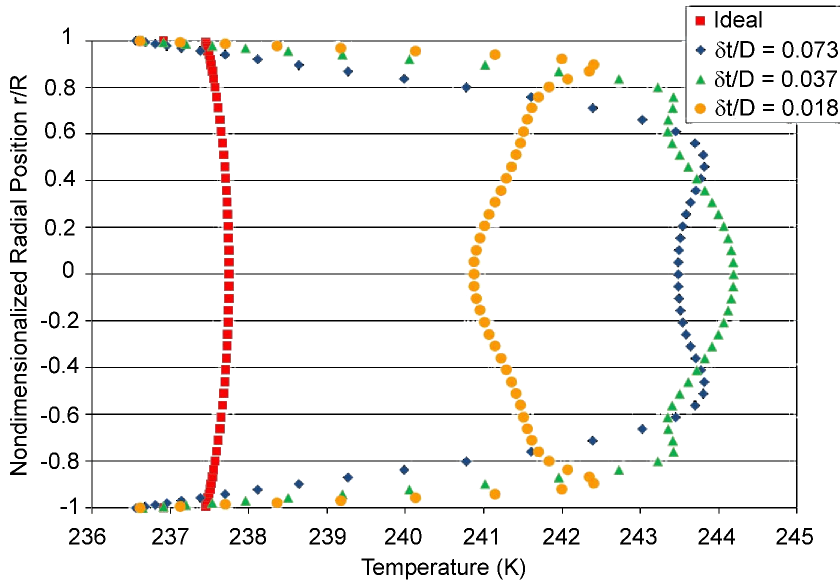**Figure 2.** Simulated instantaneous velocity profiles.



**Figure 3.** Simulated instantaneous temperature profiles.

The results in Figures 2, 3, and 4 display the ability of the CFD models to capture the expected thermal and viscous boundary layer phenomena and also demonstrate the minimal presence of these phenomena in the ideal cases. The ideal cases may therefore be used for separating the losses attributable to the boundary layers from those which would occur regardless of their presence. For all of the cases, net and gross cooling rates were evaluated from the cycle-averaged enthalpy flow rates at the warm and cold ends of the pulse tube, respectively, labeled $<H_{whx}>$ and $<H_{chx}>$ in Figure 1. The boundary layer loss for each model was defined as the difference between its predicted net cooling rate and that of the corresponding ideal case. The model's gross cooling rate was then used to normalize the boundary layer loss.
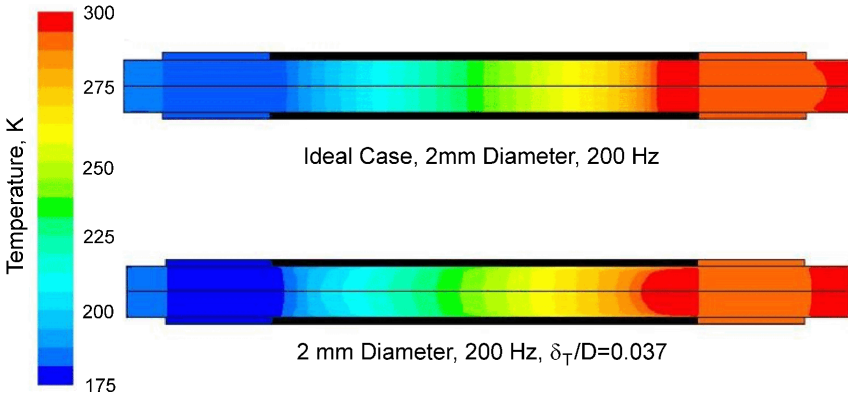
**Figure 4.** Simulated temperature contours.

The results of the CFD models are presented in this form in Figure 5. Predicted boundary layer losses, normalized by the corresponding gross cooling rates, are plotted as a function of thermal boundary layer thickness divided by the pulse tube diameter ($d_T$/D). The results show that the simulated boundary layer loss increases nearly linearly with $\delta_T$/D, ranging from less than 10% to 70% of the maximum available heat lift. Losses of approximately 10%, calculated for $\delta_T$/D below 0.02, are considered typical for conventional scale PTCs and are likely acceptable for miniaturized PTCs as well. The higher losses predicted as $\delta_T$/D approaches 0.1, however, would likely be prohibitive to obtaining useful cryogenic refrigeration.

## CONCLUSIONS

A numerical parametric study was performed to determine the effects of the thermal and viscous boundary layer thicknesses as they increased relative to the pulse tube diameter in a miniature PTR. Pulse tube diameters of 1, 2, and 4 mm and frequencies of 100 – 400 Hz were modeled to produce results over a range of $\delta_T$/D and $\delta_V$/D values from approximately 0.01 to 0.1. Ideal models
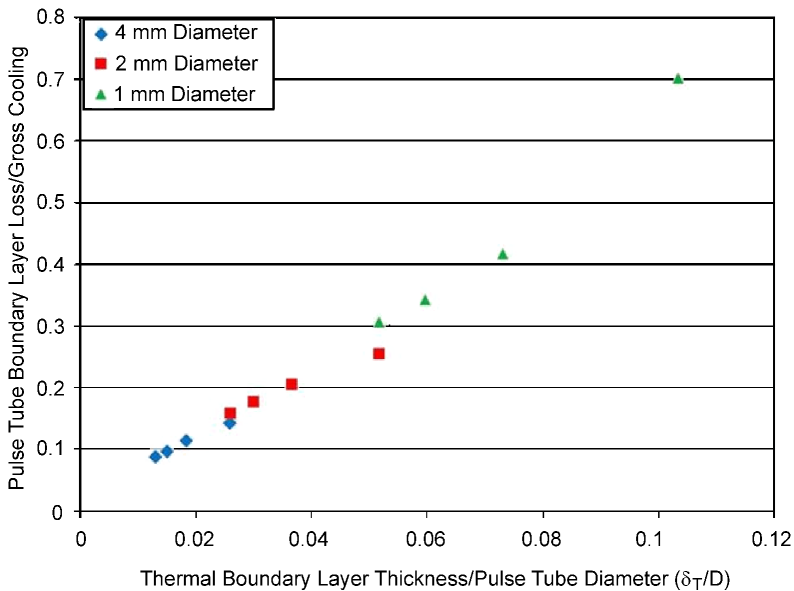


**Figure 5.** Normalized pulse tube boundary layer loss vs. $\delta_T$/D.

were also constructed for which boundary layer effects were expected to be negligible. The results of these ideal simulations indicated essentially uniform 1-D flow; therefore, the predictions of these models were used to separate the losses attributable to the boundary layers form those which would occur regardless of their presence. The boundary layer losses were then separated and normalized by the calculated gross cooling for each model and plotted against $\delta_T/D$. The results indicated that the predicted boundary layer loss increases as the boundary layer thicknesses increase relative to the pulse tube diameter. As $\delta_T/D$ increases to 10%, the predicted boundary layer loss increases to 70% of the gross cooling, a level of loss which would likely prevent useful cooling in a miniature PTR. The simulation results therefore suggest that close attention must be given to the sizes of the boundary layers relative to the pulse tube physical dimensions when designing miniature pulse tube cryocoolers.

## REFERENCES

1.  Gifford, W.E., Longsworth, R.C., "Pulse Tube Refrigeration," Transactions of the ASME Journal of Engineering for Industry, 1964.

2.  Mikulin, E.I., Tarasov, A.A., Shkrbyonock, M.P., "Low Temperature Expansion Pulse Tubes. Advances in Cryogenic Engineering," *Adv. in Cryogenic Engineering,* Vol. 29, Plenum Publishing Corp., New York (1984), pp. 629-637.

3.  Radebaugh, R., Zimmerman, J., Smith, D.R., and Louie, B., "A Comparison of Three Types of Pulse Tube Refrigerators: New Methods for Reaching 60K," *Adv. in Cryogenic Engineering,* Vol. 31, Plenum Publishing Corp., New York (1986), pp. 779-789.

4.  Lee, J., Kittel, P., Timmerhaus, K., and Radebaugh, R., "Steady Secondary Momentum and Enthalpy Streaming in the Pulse Tube Refrigerator," *Cryocoolers 8*, Plenum Press, New York (1995), pp. 359-367.

5.  Conrad, T.J., Landrum, E.C.,Ghiaasiaan, S.M., Kirkconnell, C.S.,Crittenden, T., Yorish, S., "CFD Modeling of Meso-Scale and Micro-Scale Pulse Tube Refrigerators," *Cryocoolers 15*, ICC Press, Boulder, CO (2009), pp. 241-248.

6.  Garaway, I., Grossman, G., "A Study of High Frequency Miniature Reservoir-less Pulse Tube," *Adv. in Cryogenic Engineering*, Vol. 53, Amer. Institute of Physics, Melville, NY (2008), pp. 1547-1554.

7.  Garaway, I., et. al., "Development of a Miniature 150 Hz Pulse Tube Cryocooler,"*Cryocoolers 15*, ICC Press, Boulder, CO (2009), pp. 105 - 113.

8.  Thermophysical Properties of Fluid Systems. Available at: http://webbook.nist.gov/chemistry/fluid/.

9.  Fluent 6 User Manual, Fluent Inc. 2003.

10. Conrad, T.J., Ghiaasiaan, S.M., Kirkconnel, C.S., and Crittenden, T., "Impact of Small Regenerator Structural Flaws on the Performance of Miniature Pulse Tube Cryocoolers," *Cryocoolers 16*, ICC Press, Boulder, CO (2011), (this proceedings).

11. Conrad, T.J., Landrum, E.C.,Ghiaasiaan, S.M., Kirkconnell, C.S.,Crittenden, T., Yorish, S., "Anisotropic Hydrodynamic Parameters of Regenerator Materials Suitable for Miniature Cryocoolers," *Cryocoolers 15*, ICC Press, Boulder, CO (2009), pp. 343 - 350.